Article

Journal of Chemical Research

Journal of Chemical Research
1–7

DOI: 10.1177/17475198211001819
journals.sagepub.com/home/chl
SAGE

L-ascorbyl 6-palmitate as lead compound targeting SphK1: an in silico and in vitro investigation

HaiJiao Chen[1*], Xinmei Yang[2*], Peng Sun[1], Ying Zhi[1], Qingqiang Yao[1] and Bo Liu[1]

Abstract

Sphingosine kinases (SphKs) are a class of lipid kinases, that have received extensive attention as important rate-limiting enzyme in tumor. Inhibition of the activity of SphK1 can lead to an anticancer effect. Herein, we describe the discovery process and biological characteristics of a new SphK1 inhibitor, ascorbyl palmitate, discovered through computer-aided drug design. Biochemical experiments show that ascorbyl palmitate has a strong inhibitory effect on SphK1, with an IC_{50} value of 6.4 μM. The MTT experiment showed that ascorbyl palmitate had anti-cancer effects toward the U87, A549, 22RV1, and A375 cell lines. Among them, ascorbyl palmitate has prominent inhibitory activity against the 22RV1 cell line, with an IC_{50} value of 41.57 μM. To explore the structure–activity relationship, four ascorbyl palmitate derivatives were synthesized and tested for kinase activity. The outstanding effect of ascorbyl palmitate toward SphK1 and its known non-toxicity suggest that ascorbyl palmitate may be a lead compound for the development of effective SphK1 anti-cancer inhibitors.

Keywords

anti-cancer, ascorbyl palmitate, inhibitors, sphingosine kinase, virtual screening

Date received: 20 February 2021; accepted: 22 February 2021

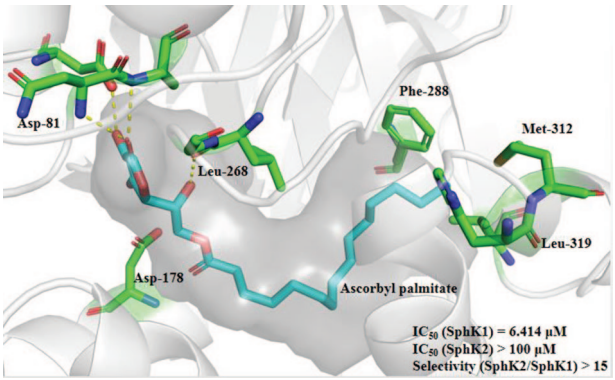

[1]Institute of Materia Medica, Shandong First Medical University & Shandong Academy of Medical Sciences, Jinan, P.R. China
[2]Department of Clinical Pharmacy, The First Affiliated Hospital of Shandong First Medical University & Shandong Provincial Qianfoshan Hospital, Jinan, P.R. China

*These authors contributed equally.

Corresponding authors:
Qingqiang Yao, Institute of Materia Medica, Shandong First Medical University & Shandong Academy of Medical Sciences, Jinan 250117, Shandong, P.R. China.
Email: qqyao@sdfmu.edu.cn

Bo Liu, Institute of Materia Medica, Shandong First Medical University & Shandong Academy of Medical Sciences, Jinan 250117, Shandong, P.R. China.
Email: mls_liub@ujn.edu.cn

Introduction

Sphingosine kinases (SphKs), as lipid kinases, have two different subtypes (SphK1/SphK2). They are closely related to the occurrence and development of cancers.[1] They participate in the progression of cancers in two different ways: one is the role of SphKs as an oncogene,[2] and the other is the role of their metabolite sphingosine-1-phosphate (S1P).[3] They are involved in the regulation of a variety of signaling pathways through the production of S1P, which mediates a variety of biological functions such as calcium mobilization, mitogenesis, apoptosis, cell motility, and angiogenesis. Reducing the production of S1P by inhibiting SphKs can inhibit the occurrence and development of some diseases.[4] As far as SphK1 is concerned, it has been shown to be highly expressed in a variety of cancer cells such as ovarian, cervical, colon, stomach, lung, and brain cancer.[5,6] Overexpressed SphK1 can not only stimulate cell growth but also cause malignant transformations of normal cells.[7] In contrast, SphK2 is much more complicated, and its effect on cells mainly depends on the degree of overexpression of SphK2.[8] Also, due to the uncertainty of the structure and function of SphK2, SphK1 inhibitors are still more frequently used.[9] In recent years, SphKs inhibitors have been studied; some of which have entered clinical trials.[10] For example, ABC294640 has an inhibitory effect on the growth of prostate cancer and colorectal cancer, is also effective for other solid tumors, and has completed a phase I clinical trial (NCT01488513).[11] There are some excellent SphK1 inhibitors, such as PF-543, Com23, Com83, SKI-II, Com54, SK1-I, and SKI-178 (Figure 1).[12,13]

Computer-aided drug design has been recognized as an important tool for the discovery of drugs.[14] Structure-based virtual screening is a common technique used by most pharmaceutical companies as well as certain academic groups in the early stages of drug development. Analysis of various SphK1 protein crystal structures also provides convenience for the virtual screening of SphK1 inhibitors. The crystal structure of the SphK1 protein was first reported in 2013.[15] It was proposed that there is a polar head and a hydrophobic tail in the SphK1 protein cavity, and the key amino acids Asp81, Leu268, and Asp178 play a key role in the polar part. Therefore, in this study, we used the SphK1 inhibitors mentioned above (Figure 1) to construct some pharmacophore models, and the pharmacophore models are then evaluated. The compound library was initially screened using the optimal pharmacophore model, and then the selected compounds were molecularly docked with SphK1 (3vzb). Finally, in order to obtain potential SphK1 inhibitors, the compounds with the best docking scores were tested for SphK1 kinase activity. Figure 2 shows a flowchart of the virtual screening.

Results and discussion

Establishment and evaluation of the pharmacophore model

In this study, all operations related to computer-aided drug design were performed with BIOVIA Discovery Studio 2020 (DS2020). First is the construction and validation of pharmacophore models. Based on the principle of the diversity of active molecular structures of a training set, seven SphK1 antagonists with high activity reported in the literature were selected to construct the pharmacophore models. The training set is shown in Figure 1. The construction and evaluation of the pharmacophore model refer to earlier reports.[16,17] The Supporting Information provides the detailed process of the pharmacophore model construction. In this study, the hydrophobic (H) characteristics, hydrogen bond acceptor (HBA), hydrogen bond donor (HBD), and aromatic ring center (R) were selected as the characteristic pharmacophore elements. Using the Common Feature Pharmacophore Generation module of the DS2020 software, 10 models were constructed based on the active conformations of the training set molecules. Figure 3(a) shows the scoring situation of 10 models. From the scoring ranking and pharmacodynamic feature elements of Figure 3(a), we find that models 1–3 have more pharmacophore characteristics and higher rankings. In order to further evaluate the effect of these models, 15 active compounds and 15 inactive compounds (Supplemental Figure S1) were used as a testing set to evaluate these 10 models again. As shown in the heat map Figure 3(b), the pharmacophore model 3 had a high matching value with the 15 active compounds, and a low matching value with the 15 inactive compounds.[18] Figure 3(c) shows the composite diagram between model 3 and the SphK1 inhibitor PF-543. It can be found from Figure 3(c) that the polar head of PF-543 has HBA characteristics. The rest of the pharmacophore features are hydrophobic characteristics. This model coincides with the "*J*-shaped" hydrophobic cavity of SphK1. Therefore, model 3 was selected for preliminary screening of the compound library.

Virtual screening of databases

Based on the results of the pharmacophore evaluation, we chose model 3 as the optimum model to screen the Selleck database. Next, the Selleck database containing 99,040 compounds was filtered to rule out compounds that do not maintain drug-likeness and the remaining 51,020 compounds were optimized by the Prepare Ligand Procedure module in the DS2020 software. And these 51,020 compounds were virtually screened by the optimal pharmacophore model 3. According to the ranking of fit values, the top 4324 compounds were selected for molecular docking. The 100 compounds with the highest docking scores were then analyzed for interactions with SphK1. According to the interactions of the compounds with the key amino acid residues Asp81 and Asp178, 12 compounds were selected as potential SphK1 inhibitors. Figure 4 shows the structures of these 12 compounds.

Kinase inhibitory activities

These 12 compounds were tested for their inhibition rate against SphK1 at a concentration of 10 μM. Their inhibition rates on SphK1 at a concentration of 10 μM are shown in Table 1. From Table 1, it is seen that at a concentration of 10 μM, most of the compounds had no inhibitory effect on

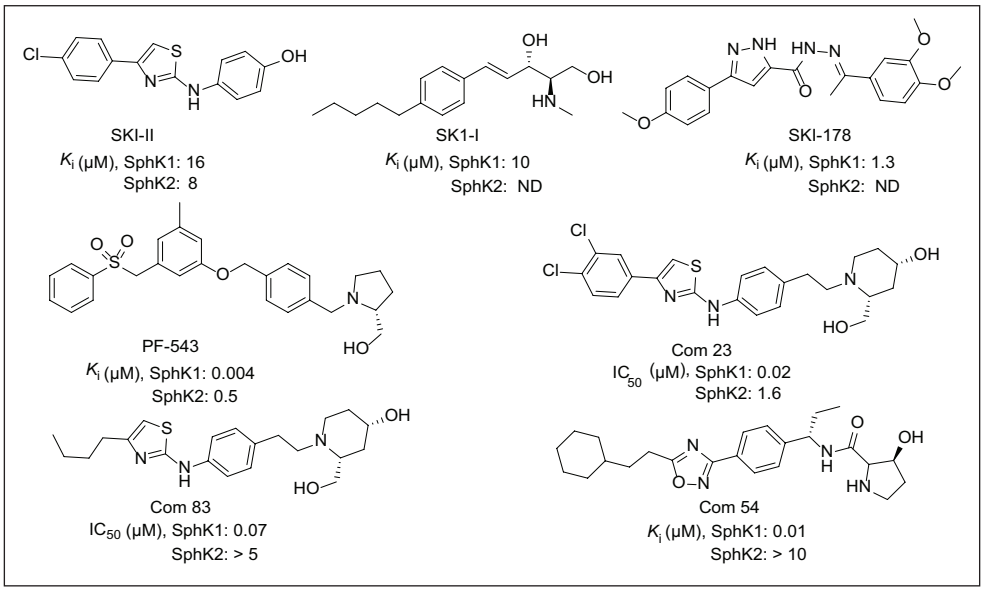

Figure 1. Examples of SphK1 inhibitors.
ND: not determined.

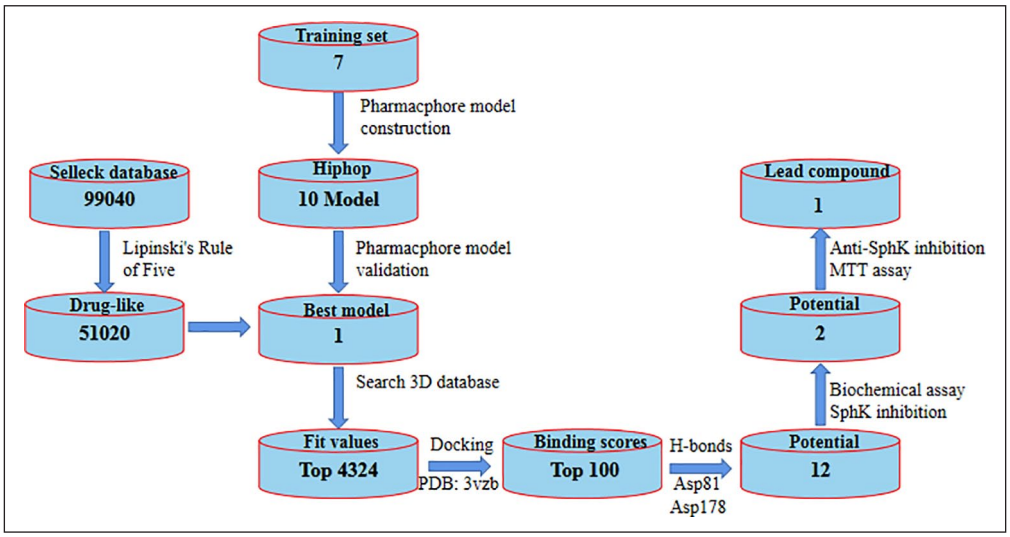

Figure 2. The flowchart of the virtual screening.

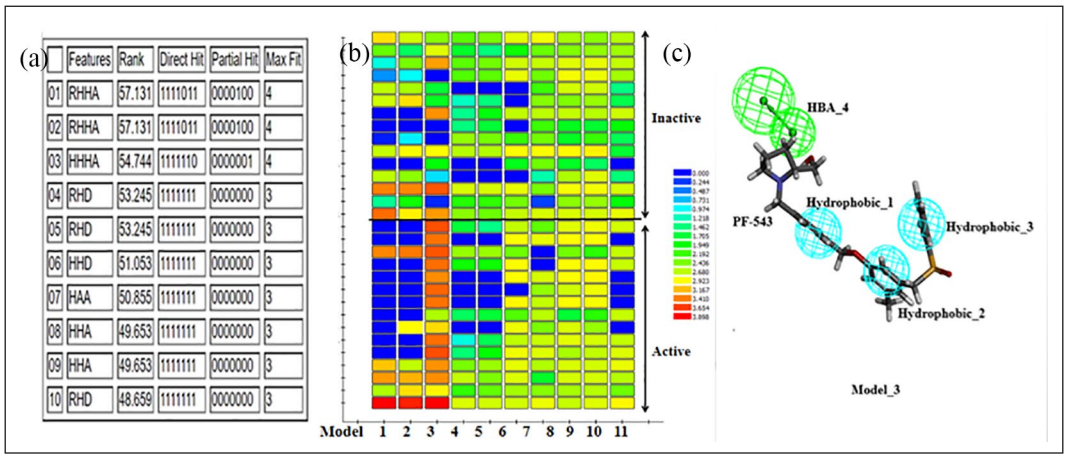

Figure 3. (a) The scores of 10 models (H stands for hydrophobic characteristics, R stands for aromatic ring center, D stands for hydrogen bond donor, and A stands for hydrogen bond acceptor). (b) The heat map of 10 models (the red square represents the higher the match between the compounds and the models). (c) The composite diagram between model 3 and PF-543 (the green ball represents the hydrogen bond acceptor (HBA), and the blue ball represents the hydrophobic characteristic).

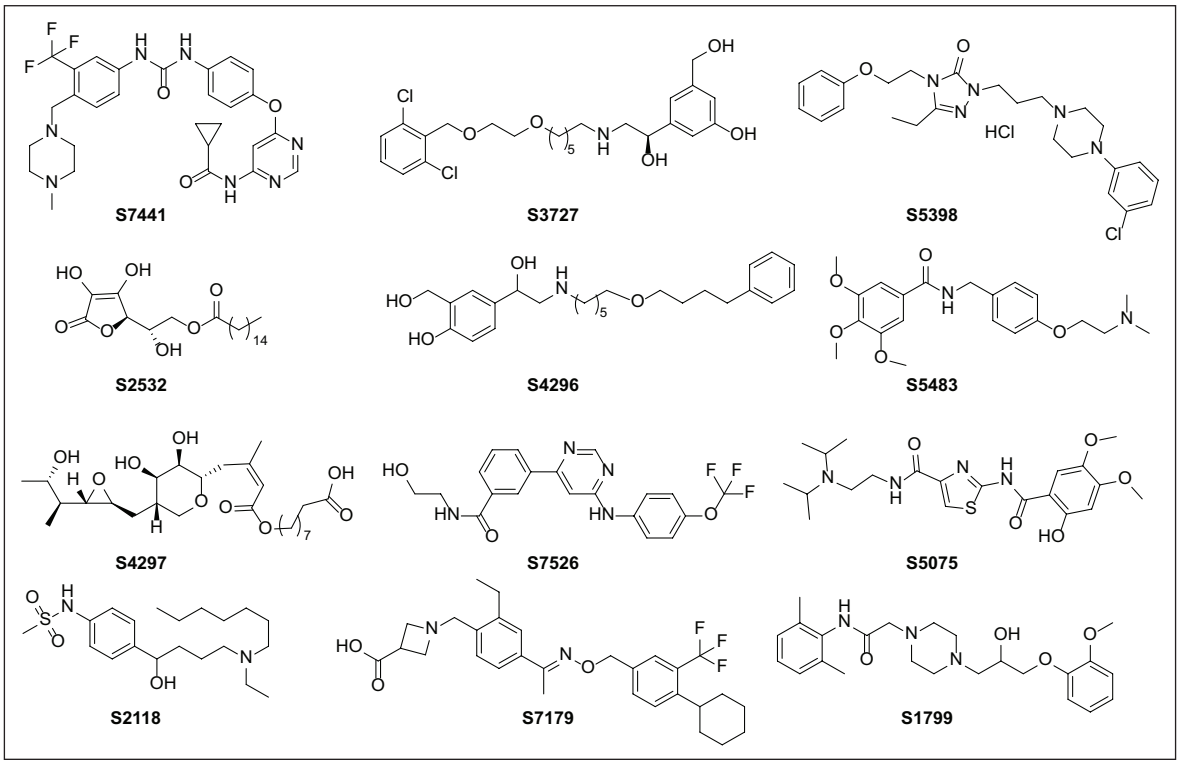

Figure 4. The structures of the 12 compounds selected for study of the inhibition of SphK1 (the number of the compound corresponds to its catalog number in the Selleck database).

Table 1. The inhibition rates of the 12 selected compounds against SphK1 at 10 μM.

Compound	Inhibition (%)[a]	Compound	Inhibition (%)
S7441	NT	**S4297**	NT
S3727	NT	**S7526**	NT
S5398	NT	**S5075**	NT
S2532	61.8	**S2118**	25.0
S4296	NT	**S7179**	NT
S5483	NT	**S1799**	NT

NT: no activity detected.
[a]Values are percent inhibitions of SphK1 at 10 μM, averages of two separate experiments, standard deviations were ±5%.

SphK1. However, the two compounds numbered **S2532** and **S2118** were outstanding, especially **S2532** which inhibited SphK1 by 61.8% at a concentration of 10 μM.

The SphKs assays were carried out as described previously.[19] From Table 1, it can be seen that the compounds numbered **S2532** and **S2118** have good SphK1 inhibitory effects. So, we continued to evaluate their IC_{50} value against SphK1 and SphK2. As shown in Table 2, compounds numbered **S2532** and **S2118** had no inhibitory effect on SphK2, and compound **S2532** has better SphK1 inhibitory activity with an IC_{50} value of 6.414 μM. This also shows that compound **S2532** is a highly selective SphK1 inhibitor.

Cytotoxic activity

From the structure of compound numbered **S2532**, we can see that it is ascorbyl palmitate (**AP**). Although **AP**, as a fat-soluble form of vitamin C (VC), is not a natural substance, its raw materials, VC and palmitic acid, are both natural ingredients. **AP** is not only harmless to the human body but also has certain nutritional properties.[20] **AP**, as an anti-cancer compound, has attracted widespread interest due to its lipophilicity, which allows it to easily pass through cell membranes.[21] But so far, there is no report that it has an inhibitory effect against SphK1. It is known that cells with high SphK1 expression are distributed in glioma, melanoma, prostate cancer, lung cancer, and liver cancer. So, these five cell lines were used to test the cytotoxic activity of **AP**. Table 3 shows that **AP** does not exhibit strong anti-cancer effects compared to cisplatin, but it had certain anti-cancer effects toward the U87, A549, 22RV1, and A375 cell lines. Among them, **AP** has a prominent inhibitory activity against the 22RV1 cell line, with an IC_{50} value of 41.57 μM.

Table 2. The inhibitory effects of compounds numbered **S2532** and **S2118** against SphKs.

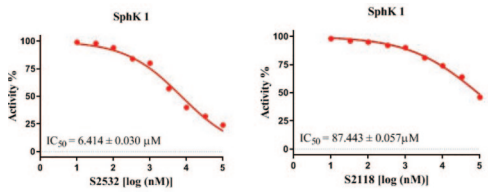

Compound	IC_{50} (μM)		Selectivity (SphK1/SphK2)
	SphK1	SphK2	
S2532	6.414 ± 0.030	>100	15.59
S2118	87.443 ± 0.057	>100	1.14
PF-543	0.052 ± 0.007	6.1	117

Table 3. Anti-proliferative effects of **AP**.

Compound	IC_{50} (μM)				
	U87	A549	22RV1	A375	HepG2
AP	63.92 ± 5.31	46.19 ± 3.16	41.57 ± 4.51	54.47 ± 3.72	>100
Cisplatin	10.8 ± 0.87	6.54 ± 0.79	10.375 ± 1.63	13.785 ± 0.62	5.98 ± 1.13

AP: ascorbyl palmitate.

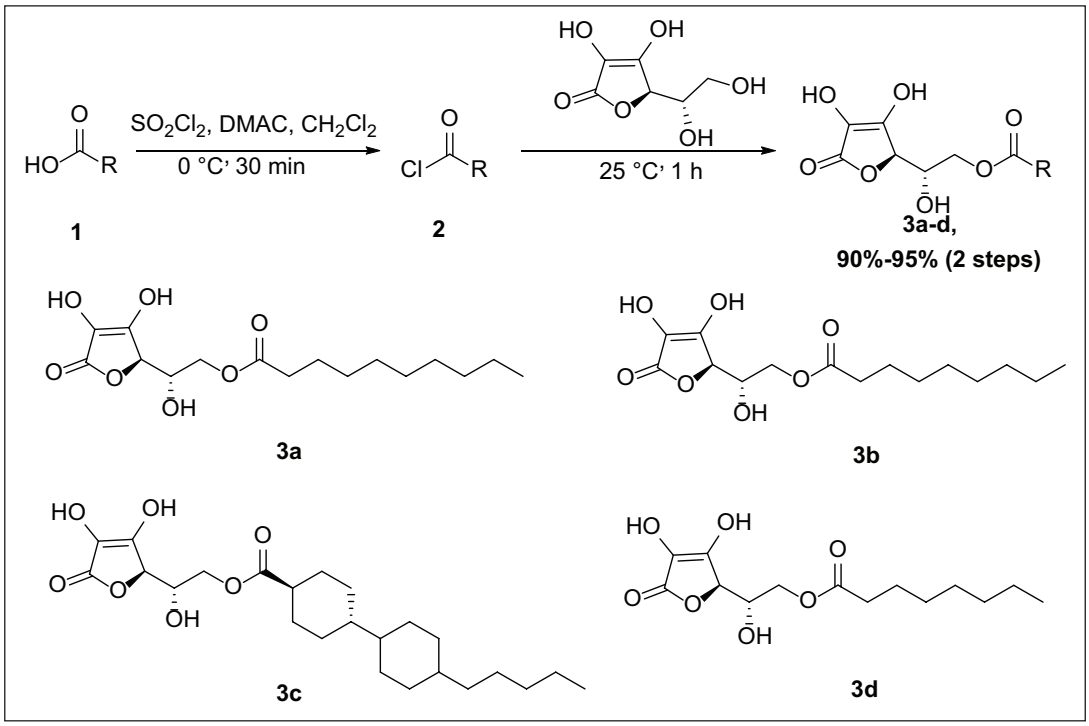

Scheme 1. Synthetic route toward **AP** derivatives **3a–d**.

Structure derivatization of AP

AP has a prominent role in inhibiting the activity of SphK1, so we used it as the lead compound for structural derivatization. The synthesis of the **AP** derivatives is shown in Scheme 1. Their synthesis was carried out using a "one-pot" method. Carboxylic acids (10 mmol), DMAC (15 mL), and CH_2Cl_2 (5 mL) were added to a flask. Next, $SOCl_2$ (13 mmol) was slowly added dropwise at 0 °C. The mixture was reacted at 10 °C for 0.5 h, and then L-ascorbic acid (12 mmol) was added. One h later, **AP** derivatives in high yield were obtained. The Supporting Information provides the complete synthetic procedure and NMR data of compounds **3a–d**.

Kinase activity of the AP derivatives *3a–d*

In order to further study the structure–activity relationship between the **AP** derivatives and SphK1, **VC** and compounds **3a–d** were preliminarily screened for SphK1 activity. Table 4 shows their inhibition rates toward SphK1 at a concentration of 10 μM. It can be seen from the table that **VC** has no inhibitory effect on SphK1, and it can only inhibit SphK1 when its side chain contains longer substitutions. This shows that, for **AP** derivatives, the terminal alkyl side chain is essential for inhibitory activity against SphK1.

Docking of **AP** *and SphK1*

We performed molecular docking analysis on the crystal structure of **AP** and the SphK1 protein. Figure 5 shows a schematic diagram of the two-dimensional and three-dimensional interactions between **AP** and SphK1. As shown in Figure 5(a), **AP** is filled in the "*J*-shaped" cavity of SphK1, and its polar head can form hydrogen bond interactions with the key amino acid residues Asp81 and Leu268. The longer alkyl side chain can also fill the cavity well. And as shown in Figure 5(b), the longer hydrophobic side chain of **AP** can form multiple hydrophobic interactions with Phe288, His311, Leu319, and Met312. Therefore, perhaps the better interaction between the entire **AP** molecule and SphK1 determines its better kinase inhibitory effect.

Conclusion

In summary, we have reported the discovery of new SphK1 inhibitors by a computer-aided virtual screening approach and biological validations. It was determined by in vitro enzymatic activity that compounds numbered **S2532** and **S2118** have the potential to inhibit SphK1 activity. Among them, compound **S2532** (**AP**) shows good SphK1 inhibitory activity and selectivity, with an IC_{50} value of 6.4 μM against SphK1. Meanwhile, **AP** reduced 22RV1 cell growth

Table 4. Inhibition studies of **AP** derivatives against SphK1 at 10 μM.

Compound	Inhibition (%)[a]	Compound	Inhibition (%)
VC	NT	**3a**	28
3b	34	**3c**	32
3d	44		

VC: vitamin C; NT: no activity detected.
[a]Values are percent inhibitions against SphK1 at 10 μM, averages of two separate experiments, standard deviations were ±5%.

with an IC_{50} value of 40 μM. Although **AP** displayed relatively poor activity compared to cisplatin, it could still be utilized as an excellent lead for the further development of SphK1 inhibitors due to its outstanding effect on SphK1 and the fact that it is known to be non-toxic.

Experimental

Materials

Vitamin C, thionyl chloride, *N,N*-dimethy-lacetamide, dichloromethane, sodium bicarbonate, fetal bovine serum, and other materials were obtained from commercial sources and were used without further purification.

Apparatus

High-resolution mass spectrometry (HRMS) was performed on an AB SCIEX X500R Accurate Mass Q-TOF using electrospray ionization (ESI). The NMR spectra were recorded on a Bruker AM-600 spectrometer (Billerica, MA, USA) with tetramethylsilane as the internal standard.

Synthesis

The synthesis of **AP** derivatives was carried out using a "one-pot" method. Scheme 1 shows the general synthetic method for the compounds **3a–d**. Carboxylic acid (10 mmol) with different substituents, DMAc (15 mL), and CH_2Cl_2 (5 mL) were added to a flask and the mixture stirred at room temperature. Next, $SOCl_2$ (13 mmol) was slowly added dropwise at 0 °C. The mixture was reacted at 10 °C for 0.5 h, and then L-ascorbic acid (12 mmol) was added. The resulting mixture was stirred, heated, and maintained at 25 °C for 1 h. A new spot appeared according to thin-layer chromatography (TLC). The reaction mixture was extracted with ethyl acetate, and the combined organic layers were washed with brine and dried over Na_2SO_4. The organic layer was filtered and concentrated under reduced pressure to dryness to provide the crude product, which was purified by silica gel chromatography to give the desired product. The Supporting Information contains the NMR data of compounds **3a–d**.

(*S*)-2-((*R*)-3,4-dihydroxy-5-oxo-2,5-dihydrofuran-2-yl)-2-hydroxyethyl decanoate (**3a**). White solid; 95% yield. ^{1}H NMR (600 MHz, CD_3OD): δ 4.73 (d, *J* = 2.01 Hz, 1H), 4.19-4.28 (m, 2H), 4.07-4.10 (m, 1H), 2.37 (t, *J* = 7.41 Hz, 2H), 1.57-1.67 (m, 2H), 1.24-1.38 (m, 12H), 0.89 (t, *J* = 6.46 Hz, 3H). ^{13}C NMR (150 MHz, CD_3OD): δ 173.76, 171.74, 152.69, 118.68, 75.81, 66.69, 64.41, 33.48, 31.62, 29.15, 28.99, 28.98, 28.77, 24.57, 22.30, 13.01. HRMS (ESI): m/z $[M + H]^+$ calcd for $C_{16}H_{27}O_7$: 331.1835; found: 331.1753.

(*S*)-2-((*R*)-3,4-dihydroxy-5-oxo-2,5-dihydrofuran-2-yl)-2-hydroxyethyl nonanoate (**3b**). White solid; 90% yield. ^{1}H NMR (600 MHz, CD_3OD): δ 4.73 (d, *J* = 2.03 Hz, 1H), 4.16-4.27 (m, 2H), 4.06-4.12 (m, 1H), 2.37 (t, *J* = 7.4 Hz, 2H), 1.59-1.68 (m, 2H), 1.25-1.39 (m, 10H), 0.90 (t, *J* = 6.43 Hz, 3H). ^{13}C NMR (150 MHz, CD_3OD): δ 174.02, 171.73, 152.65, 118.69, 75.80, 66.68, 64.43, 37.08, 32.72 (2C), 32.05, 31.10, 26.24, 25.94 (2C). HRMS (ESI): m/z $[M + H]^+$ calcd for $C_{15}H_{25}O_7$: 317.1522; found: 317.1548.

(*S*)-2-((*R*)-3,4-dihydroxy-5-oxo-2,5-dihydrofuran-2-yl)-2-hydroxyethyl (1S,4r)-4'-pentyl-[1,1'-bi(cyclohexane)]-4-carboxylate (**3c**). White solid; 94% yield. ^{1}H NMR (600 MHz, CD_3OD): δ 4.73 (d, *J* = 2.09 Hz, 1H), 4.24-4.27 (m, 1H), 4.17-4.21 (m, 1H), 4.07-4.10 (m, 1H), 3.67 (t, *J* = 4.54 Hz, 3H), 3.56 (t, *J* = 4.95 Hz, 3H), 2.37 (t, *J* = 7.43 Hz, 2H), 1.60-1.65 (m, 2H), 1.24-1.39 (m, 18H), 0.89 (t, *J* = 6.99 Hz, 3H). ^{13}C NMR (150 MHz, CD_3OD): δ 173.75, 171.73, 152.57, 118.69, 75.79, 72.12 (2C), 66.66, 64.40, 60.86 (2C), 33.47, 31.67, 29.33 (3C), 29.20, 29.06 (2C), 29.00, 28.78, 24.58, 22.33, 13.04. HRMS (ESI): m/z $[M + H]^+$ calcd for $C_{24}H_{39}O_7$: 438.2618; found: 439.2686.

(*S*)-2-((*R*)-3,4-dihydroxy-5-oxo-2,5-dihydrofuran-2-yl)-2-hydroxyethyl octanoate (**3d**). White solid; 92% yield. ^{1}H NMR (600 MHz, CD_3OD): δ 4.74 (d, *J* = 2.02 Hz, 1H), 4.17-4.28 (m, 2H), 4.07-4.11 (m, 1H), 2.37 (t, *J* = 7.43 Hz, 2H), 1.57-1.67 (m, 2H), 1.24-1.39 (m, 8H), 0.90 (t, *J* = 6.42 Hz, 3H). ^{13}C NMR (150 MHz, CD_3OD): δ 173.85, 171.76, 152.61, 118.72, 75.83, 66.74, 64.42, 33.57, 31.46, 28.78, 28.70, 24.61, 22.29, 13.13. HRMS (ESI): m/z $[M + H]^+$ calcd for $C_{14}H_{23}O_7$: 303.1366; found: 303.1433. The ^{1}H and ^{13}C NMR spectra for compounds **3a–d** in detail can be found in the Supporting Information.

The kinase test in vitro

The SphKs assays were carried out as described previously.[19] The assay was performed using Kinase-Glo Plus luminescence kinase assay kit (purchased from Promega, Fitchburg, USA). It measures kinase activity by quantitating the amount of ATP remaining in solution following a kinase reaction. Here, we used PF-543 (purchased from Selleckchem, Houston, TX, USA) as a positive control. The reaction system was 50 μL. Compounds **S2532** and **S2118** were dissolved in pure DMSO to prepare 10 mM stock solutions and diluted with Kinase buffer (pH = 7.4, composition: 40 mM L^{-1} Tris, 10 mM L^{-1} $MgCl_2$, 0.1 g L^{-1} BSA, 1 mM L^{-1} DTT, and 10 μM L^{-1} ATP). SphK1/2 was added to 96-well plates, which were then treated with desired concentrations of **S2532** or **S2118** (0.01, 0.1, 1, 10, and 100 μM) for 40 min at 30 °C. The ATP test solution was then added, and the mixtures were incubated at room temperature for 5 min. The luminescence was immediately measured using a microplate

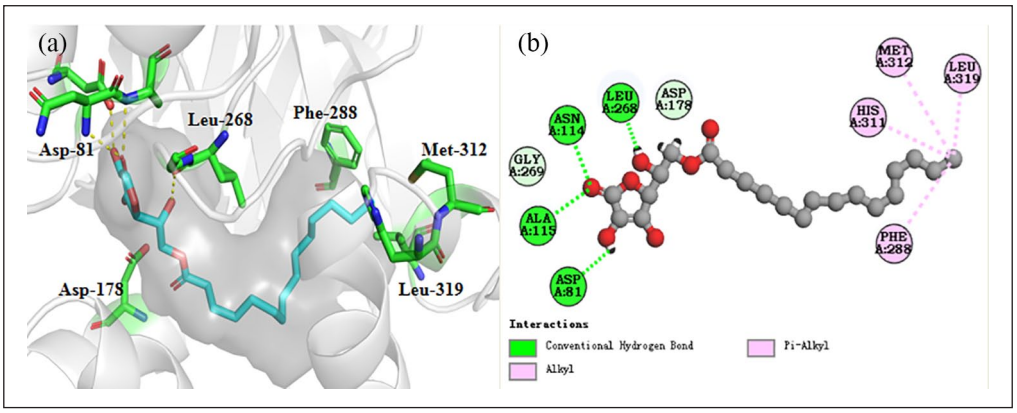

Figure 5. The schematic diagram of the three-dimensional (a) and two-dimensional (b) interactions between **AP** and SphK1. The green balls represent the hydrogen-bonding interactions, and the pink balls represent the hydrophobic interactions.

spectrophotometer (AD 340, Beckman, USA). Finally, GraphPad Prism 5 software was used to analyze the data.

Declaration of conflicting interests

The author(s) declared no potential conflicts of interest with respect to the research, authorship, and/or publication of this article.

Funding

The author(s) disclosed receipt of the following financial support for the research, authorship, and/or publication of this article: This work was supported by grants from the National Natural Science Foundation of China (grant no. 81903473) and the Academic Promotion Programme of Shandong First Medical University (no. 2019LJ003).

ORCID iD

HaiJiao Chen https://orcid.org/0000-0003-4526-714X

Supplemental material

Supplemental material for this article is available online.

References

1. Ogretmen B. *Nat Rev Cancer* 2018; 18: 33–50.
2. Neubauer HA, Pham DH, Zebol JR, et al. *Oncotarget* 2016; 7: 64886–64899.
3. Ekiz HA and Baran Y. *Int J Cancer* 2010; 127: 1497–1506.
4. Pyne S, Adams DR and Pyne NJ. *Prog Lipid Res* 2016; 62: 93–106.
5. Kim HS, Yoon G, Ryu JY, et al. *Oncotarget* 2015; 6: 26746–26756.
6. Hanyu T, Nagahashi M, Ichikawa H, et al. *Surgery* 2018; 163: 1301–1306.
7. Shida D, Takabe K, Kapitonov D, et al. *Curr Drug Targets* 2008; 9: 662–673.
8. Van Brocklyn JR, Jackson CA, Pearl DK, et al. *J Neuropathol Exp Neurol* 2005; 64: 695–705.
9. Pitman MR, Costabile M and Pitson SM. *Cell Signal* 2016; 28: 1349–1363.
10. Plano D, Amin S and Sharma AK. *J Med Chem* 2014; 57: 5509–5524.
11. Xun C, Chen MB, Qi L, et al. *J Exp Clin Cancer Res* 2015; 34: 94.
12. Schnute ME, McReynolds MD, Kasten T, et al. *Biochem J* 2012; 444: 79–88.
13. Hengst JA, Wang X, Sk UH, et al. *Bioorg Med Chem Lett* 2010; 20: 7498–7502.
14. Abdolmaleki A, Ghasemi JB and Ghasemi F. *Curr Drug Targets* 2017; 18: 556–575.
15. Wang Z, Min X, Xiao SH, et al. *Structure* 2013; 21: 798–809.
16. Wu H, Gu X, Li J, et al. *J Mol Graph Model* 2020; 96: 107527.
17. Jiang JH, Zhou H, Jiang QH, et al. *Molecules* 2018; 23.
18. Vettorazzi M, Angelina E, Lima S, et al. *Eur J Med Chem* 2017; 139: 461–481.
19. Yang H, Li Y, Chai H, et al. *Bioorg Chem* 2020; 98: 103369.
20. Smart RC and Crawford CL. *Am J Clin Nutr* 1991; 54: 1266S–1273S.
21. Zhou M, Li X, Li Y, et al. *Drug Deliv* 2017; 24: 1230–1242.